Regular Article

PHYSICAL CHEMISTRY RESEARCH
Published by the
Iranian Chemical Society
www.physchemres.org
info@physchemres.org

Phys. Chem. Res., Vol. 11, No. 1, 79-89, March 2023
DOI: 10.22036/pcr.2022.329552.2029

Performance of a Recirculating Fixed Bed Reactor for the Oxidation of Phenol and Trisubstituted Phenols by Heterogeneous Photocatalytic Process-mechanistic, Kinetic and Substituents Approach

V. Kavitha*

Department of Chemistry, Sathyabama Institute of Science and Technology, Chennai-119

(Received 13 February 2022, Accepted 8 May 2022)

A recirculating fixed bed reactor was adopted to study the mineralization efficiency of phenol and trisubstituted phenols like 2,4,6-trichlorophenol (TCP), 2,4,6-trinitrophenol (TNP), and 2,4,6-trimethylphenol (TMP) using Granular Ferric Hydroxide (GFH) as a heterogeneous catalyst in the presence of solar light. The effect of operating parameters for the fixed bed reactor namely column bed height and recirculating flow rate were optimized for 2.12 mM of phenol as a model compound at pH 3.0 and 18.3 mM of hydrogen peroxide. Maximum mineralization efficiency of around 96% was attained within 2 h of the reaction time at the optimum condition of 5 cm bed height and a recirculating rate of 210 ml h^{-1}. The mineralization rate of the trisubstituted phenols follows the following order: TNP > Phenol > TMP > TCP. Higher mineralization efficiency was observed due to the synergetic effect of both photocatalysis and photo-Fenton reaction. The electron withdrawing group in TNP facilitates the higher mineralization efficiency and its rate constant is increased by a factor of 2 compared to the electron donating group in TMP. The electronegativity of chlorine together with the scavenging effects of chloride ions decreases the efficiency of TCP by a factor of 2.7 as compared to TNP.

Keywords: Granular Ferric Hydroxide (GFH), Recirculating flow reactor, Photo-Fenton process, Photocatalysis, Hammett constants

INTRODUCTION

Phenols and it's their substituents mainly trisubstituted phenols are listed among 129 priority pollutants by the United States Environmental Protection Agency (USEPA) as they are toxic, persistent, and recalcitrant in nature. These compounds constitute a potential threat to the ecosystem and human health. Conventional treatment methods like adsorption and chemical oxidation have their own limitations in removing these compounds from the water matrix as they are resistant to oxidation. Most of these compounds are efficiently removed ~~u~~nder room conditions or by using visible light by application of either Fenton process (a mixture of Ferrous ion and hydrogen peroxide). In Fenton's process, the ferrous iron in the presence of hydrogen peroxide at pH 3.0 ± 0.2 generates a highly oxidative, non-selective, and transient hydroxyl radical (·OH) as the primary oxidant for the destruction and mineralization of organic compounds [1]. However, in Fenton process, the removal of iron sludge poses serious limitations in its application to the industrial wastewater treatment process. In order to reduce the iron load in the treatment process, the Ferric ions (Fe^{3+}) generated by the decomposition of H_2O_2 undergo photochemical reactions which initiate the Fe^{3+}/Fe^{2+} cycle in the heterogeneous photo-Fenton process thereby improving the degradation of organic compounds [2]. However, in the photo-Fenton process, the photogenerated electrons and holes undergo

*Corresponding author. E-mail: kavi7511@gmail.com

recombination thereby limiting the efficiency of the process. Hence, it is essential to develop a catalyst that efficiently suppresses the recombination reaction and also prevents the leaching of iron from the catalyst. In the last decade, a new efficient catalyst has been developed by immobilizing iron onto the solid support like mesoporous silica [3], Al-Fe pillared interlayered clays [4], iron-TiO_2 [5], Zinc Ferrites [6], layered iron hydroxides [7], iron perovskites like $EuFeO_3$ [8], $LaFeO_3$ [9], by using minerals like goethite [10-11], iron oxides [12], or commercial granular ferric hydroxide [13]. In recent years, review papers have focused on the usage of natural iron-based minerals [14], semiconductors supported on iron catalyst [15], and on improving the ways to enhance the redox iron cycle [16] for the process. In these processes, iron is not dissolved in aqueous media [17-19] and exhibits its oxidation nature only in the presence of light and hydrogen peroxide thereby considered heterogeneous photo-Fenton process.

Most of the heterogeneous photo-Fenton processes reported for the removal of phenolic compounds were carried out in a batch mode. The present study exploits the possibility of using recirculating flow reactor in treating refractory phenolic compounds by the heterogeneous photo-Fenton process as these reactors achieve steady-state conditions at a faster rate. In our previous study reported, granular ferric hydroxide (GFH) exhibits negligible leachability of iron and is used as a source of iron catalyst for heterogeneous photo-Fenton system in a batch reactor [13]. Hence, in the present study also, GFH is used as a catalyst in a flow-type reactor thereby reducing the secondary iron sludge waste. The operating parameters like column bed height and the recirculating flow rate were studied using phenol as a model compound. The efficacy of the flow reactor was studied by varying the substituent in phenolic compounds from the electron-withdrawing group ($-NO_2$) to the electron releasing group ($-CH_3$) and an electronegative group (-Cl, deactivators) which explores the substituent effect in terms of mineralization of the phenolic compound. Based on mineralization rate, constant data, the reactivity, and the reaction mechanism of the hydroxyl radical towards different phenolic compounds were assessed by structural activity-relationships. Moreover, efforts have been made to give an insight into the possible mechanism for the degradation of the trisubstituted compounds together with the identification and quantification of the stable intermediates

MATERIALS AND METHODS

Chemicals and Reagents

Analytical grade reagents, Phenol S.D fine chemicals, linear formula C_6H_5OH), s-trichlorophenol (TCP) (Fluka, linear formula $C_6H_2OHCl_3$) s-trinitrophenol (TNP) (BDH, linear formula $C_6H_2OH(NO_2)_3$), s-trimethylphenol (TMP) (Lancaster, linear formula $C_6H_2OH(CH_3)_3$) in which the substituents are in 2,4,6 position were used as such without any further purification. The stock solutions of phenolic substances were prepared in 0.1 M NaOH. The initial concentration of phenolic substances during the experimental runs was 200 mg l^{-1}. The stock solution of H_2O_2 of 6.7-6.9 M was prepared by diluting 30% w/v (Qualigens make) and stabilized at acidic pH. Granular Ferric Hydroxide (GFH) was used as a source of iron in heterogeneous photo-Fenton reaction. It was purchased from Wasserchemie Gmbh & Co. KG (Germany) and marketed as a trademark of GEH®102. GFH contains 52-57% β-FeOOH and $Fe(OH)_3$ with a particle size of 0.32-2 mm while its specific area is 250-300 m^2 g as specified by the manufacturer. The point of zero-charge for GFH was determined by the solid addition method and was found to be 4.6 ± 0.1. The solar intensity and luminance during the experimental run were in the range of 780-843 W m^{-2} and 90-94 Klx respectively.

Recirculating Flow Reactor

A recirculating flow reactor used for the experimental run is depicted in Fig. 1. A stock tank of 5 l capacity containing phenolic solution and peroxide was maintained at pH 3.0 ± 0.2. A stopper was attached at 2.5 cm from the bottom of the storage tank. The outlet of the stock tank was connected to a recirculating tank fitted with a draining stopper. The outlet of the recirculating tank was fed into a glass column of 30 cm in height and an internal diameter of 2.5 cm, filled with GFH. The draining port was placed at the bottom of the glass column. Loosely packed glass wool was placed at 1 cm height from the bottom of the column and a known amount of approximately 30-80 g of GFH was transferred to the column. The columns were tapped

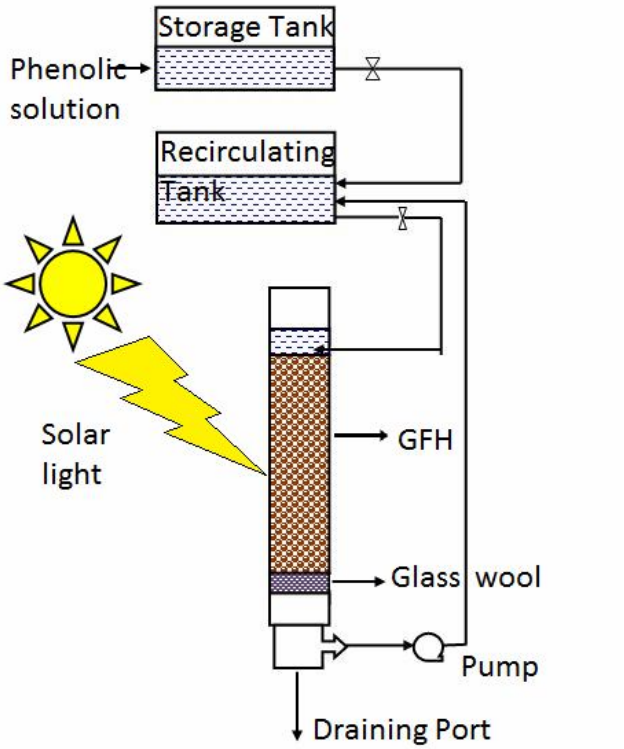

Fig. 1. Recirculating fixed bed reactor for heterogeneous process using GFH.

to avoid any dead pockets, to obtain uniform packing. The flow rate from the tanks was adjusted by placing a regulating valve and the outlet from the column was circulated to the recirculation tank using a peristaltic pump (Watson and Marlow 313S). The whole experimental setup was exposed to sunlight during the experimental run. During the experiments, a 2.5 cm solution-head was maintained over the GFH catalyst to prevent it from drying on exposure to direct solar light.

Analytical Methods

Samples were withdrawn from the draining port at specified intervals and analyzed immediately without any storage for dissolved organic carbon (DOC) and the presence of stable intermediates like oxalic acid, and acetic acid formed during the reaction. The DOC concentration in the sample was determined by quenching the reaction with 15% phosphoric acid to remove any inorganic carbon. The mineralization efficiency was monitored by the decrease in DOC content using a TOC analyzer, Analytik Jena Model 1997 equipped with liquid autosampler ALS-C-104.

$$\text{Mineralization efficiency (\%)} = (C_o - C_t/C_o) \times 100 \quad (1)$$

where C_o is the initial DOC content of the phenolic solution in mg l^{-1} and C_t is the DOC content of the phenolic solution in mg l^{-1} at time t (min). The stable intermediates like oxalic acid, acetic acid, and inorganic anions like chlorideand nitrate were quantified by an ion-chromatographic system (Dionex DX120) provided with an Ion Pac AS-14 column. Aqueous solutions of 3.5 mM Na_2CO_3 and 1.0 mM $NaHCO_3$ were used as eluents and operated at isocratic mode with a flow rate of 1.2 ml min^{-1} for the ion-chromatographic system [20]. The peaks were detected at 2.72, 3.15, and 4.25 (± 0.2) min for acetic acid, chloride, and nitrate respectively.

RESULTS AND DISCUSSION

Optimization of Flow Reactor

Preliminary studies for the mineralization of 2.12 mM of phenol indicate that GFH serves as a catalyst for photocatalysis and photo-Fenton process as described in our previous literature for batch mode [13]. The synergetic effect of photocatalysis and the photo-Fenton process is illustrated in Fig. 2. On absorbing the solar light by GFH results in the generation of holes and electrons. The electrons react with GFH to form ferrous ions which catalyze the decomposition of H_2O_2 to form ·OH radical.

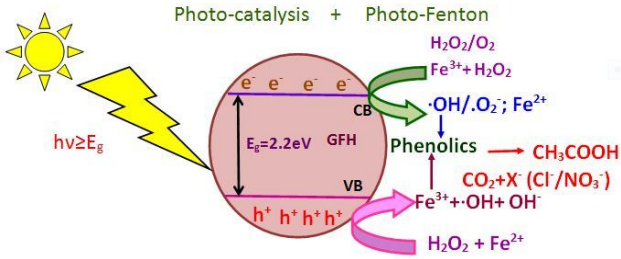

Fig. 2. Schematic representation for mineralization of phenolic compounds by heterogeneous process on GFH surface.

The holes oxidise the pollutants along with the Fenton reaction by the generation of ·OH radical, propagates the oxidation of phenolics to products [21-23]. The optimum conditions like pH of 3.0 ± 0.2 and 18.3 mM H_2O_2, adopted in the batch mode are used for the study in the recirculating reactor. The effect of vital operating parameters in the recirculating reactor namely, recirculation flow rate and column bed height were optimized using phenol as a model compound.

Effect of the Recirculation Flow Rate

A series of experiments were conducted to determine the optimum recirculation rate by varying the flow rate from 120 ml h^{-1} to 600 ml h^{-1}. In these experiments, a column bed height of 5cm was maintained which corresponds to 40 g of the GFH catalyst. As seen from Fig. 3A, decreasing the flow rate has a significant influence on the mineralization of phenol. The decrease in flow rate increases the adsorption of phenol molecules on the active sites leading to increased mineralization. The mineralization efficiency decreased with increasing flow rate with a maximum efficiency of 96% achieved at 210 ml h^{-1}. At 600 ml h^{-1}, the mineralization efficiency for phenol was only 47% at 2h time interval. During these experiments, neither iron in the +2 oxidation state nor +3 oxidation was identified in the samples indicating that photo dissolution of iron oxide leading to leaching of iron from the surface does not take place.

Effect of the Column Bed Height

The effect of GFH column bed height was determined by using different amounts of catalyst ranging from 20-80 g which occupied around 2.5 cm to 10 cm in the glass column at a recirculating rate of 210 ml h^{-1} and is depicted in Fig. 3B. An increase in the bed height from 2.5 cm to 5.0 cm increased the mineralization efficiency from 86% to 95%. With further increase in bed height, the mineralization efficiency remained the same and is found to be 96%.

Photo-oxidation of Phenolics in a Rrecirculating Flow Reactor

The performance efficiency of the recirculating flow reactor was investigated for trisubstituted phenolic compounds and phenol. Phenolic solution (200 mg l^{-1})

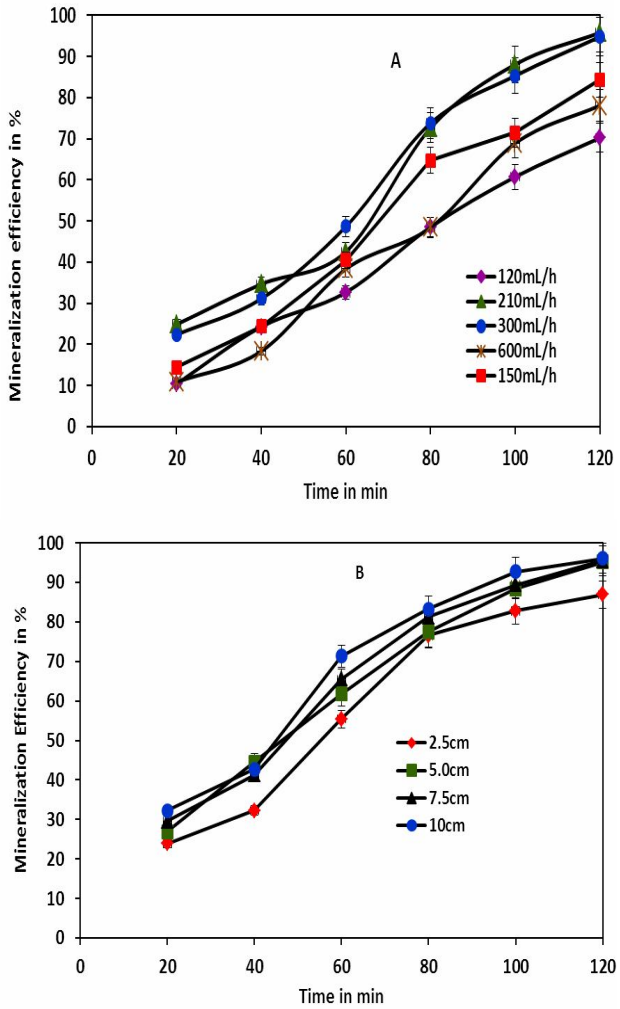

Fig. 3. Effect of recirculating flow rate (A) and column bed height (B) for the mineralization of phenol by heterogeneous process. (Experimental conditions: [Phenol] = 2.12 mM; [H_2O_2] = 18.3 mM; pH = 3.0 ± 0.2) for A- conditions are the same with a column bed height of 5 cm. For B- conditions are the same with a recirculating flow rate of 210 ml h^{-1}.

containing peroxide was allowed to pass through the column containing GFH fixed at a bed height of 5cm and a recirculation rate of 210 ml h^{-1}. Samples were withdrawn from the draining port at a time intervals of 20 min and analyzed for DOC and their intermediates.

The mineralization efficiency of TCP, TMP, TNP, and phenol is presented in Fig. 4A and is found to be 76%, 89%,

98%, and 97% respectively. The observed mineralization was due to the photocatalytic activity of GFH which leads to the formation of hydroxyl radical (·OH). The difference in mineralization efficiency may be attributed to their susceptibility of the substituents towards photo-oxidation. In TNP, mineralization efficiency, > 75% was attained within 1 h of the reaction due to the presence of three nitro groups which facilitates the faster oxidation reaction of the aromatic ring. Between 1 to 2 h of the reaction time (TNP), only 23% mineralization efficiency was achieved which reveals the resistant nature of aliphatic compounds like acetate ions formed by the fission of the aromatic phenolics. Mineralization efficiency of 48% was achieved within 1h of the reaction time in the case of TMP, as the reaction progressed between 1 to 2 h, the efficiency of 40% was noticed which can be attributed to the slow conversion of methyl groups to acetate ions which further mineralize to CO_2. Low mineralization efficiency of 76% was observed in TCP may be due to the recalcitrant nature of symmetrical-3 chlorine atoms, retarding the attack of hydroxyl radical towards the phenolic ring structure.

During the photo-Fenton reaction, low molecular weight compounds like acetic acid [24] and inorganic anions like chloride and nitrates are identified and their concentration profiles are shown in Figs. 4B and 4C. The concentration of acetic acid increases during the initial stages of the reaction and then decreases as indicated in Fig. 3C due to photolysis of ferric acetate complexes at pH 2-4 [25]. The complex undergoes a series of photochemical reactions in the UV-Vis range of 250-480 nm through ligand to metal charge transfer reactions (LCMT) thereby leading to the mineralization of organic complexes as shown in the equation [2-5,26]

$$[Fe^{3+}(C_2H_3O_2)_3]^{3-} + h\nu \longrightarrow [Fe^{2+}(C_2H_3O_2)_2]^{2-} + C_2H_3O_2^{\cdot -} \quad (2)$$

$$C_2H_3O_2^{\cdot -} + O_2 \longrightarrow 2CO_2 + O_2^{\cdot -} \quad (3)$$

$$O_2^{\cdot -} + 2H^+ \longrightarrow H_2O_2 \quad (4)$$

$$H_2O_2 + h\nu \longrightarrow \cdot OH \quad (5)$$

The presence of acetic acid and inorganic ions indicates the degradation of phenolic compounds by heterogeneous photo-Fenton process. Complete mineralization was not achieved in the case of TCP and TMP suggesting the presence of a minor amount of organic compounds remaining in the reaction media. The concentration of acetate ions reaches a maximum of 0.6-0.9 mM at different time intervals irrespective of the substituents which reveal that the formation of acetate ion occurs from the fission of

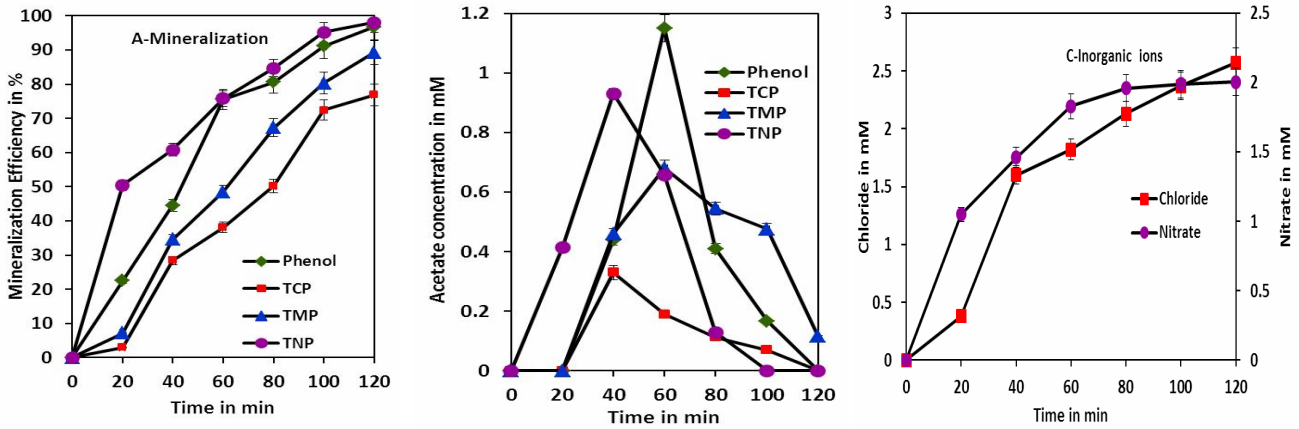

Fig. 4. Heterogeneous process for the removal of phenol and trisubstituted phenols. A- Mineralization of phenols B- Intermediates C- Inorganic ions, Chlorides and Nitrates (Experimental conditions: [Phenol] = 2.12 mM; [TCP] = 1.01 mM; [TMP] = 1.47 mM; [TNP] = 0.87 mM; [H_2O_2] = 18.3 mM; pH = 3.0 ± 0.2; column bed height = 5 cm; recirculating flow rate = 210 ml h^{-1}).

the aromatic phenyl ring. The concentration of inorganic ions like chloride and nitrate (from the degradation of TCP and TNP) is monitored and is shown in Fig 3C. The concentration of chloride ion and nitrate ion increases as the reaction progressed and reaches a maximum value of 2.32 mM and 1.92 mM respectively. Near stoichiometric amount of nitrate ion was accounted for TNP degradation while around 76% of stoichiometric organic bound chlorine was accounted as inorganic chloride during TCP degradation. The remaining stoichiometric chloride ion can be associated with oxidized chlorinated intermediate compounds which supports the presence of residual DOC in the reacting media.

Kinetics for Phenol and Trisubstituted Phenol

Hydroxyl radical (·OH) with a high oxidation potential of 2.8V (with respect to Standard hydrogen electrode) acts as a critical oxidizing agent for the degradation of phenolic compounds. The hydroxyl radical attacks the phenolic compounds to form intermediates which further react to form degraded compounds and CO_2. The overall mineralization of phenolic compounds can be represented in the following Eqs. (6)-(8).

$$\text{Phenolic compounds} + \bullet OH \xrightarrow{h\upsilon} \text{Oxidized aromatic intermediate} \quad (6)$$

$$\text{Oxidized aromatic intermediates} + \bullet OH \xrightarrow{h\upsilon} \text{Aliphatic intermediates} + CO_2 + H_2O + Cl^- + NO_3^- \quad (7)$$

$$\text{Aliphatic intermediates (Dicarboxylic acids)} + \bullet OH \xrightarrow{h\upsilon} CO_2 + H_2O + Cl^- + NO_3^- \quad (8)$$

The kinetics for the oxidation of phenolic compounds can be represented as the decrease in the reactant (phenolics) concentration as,

$$-dC_{Ph}/dt = -k_{Ph}.C_{Ph}.{}^{\cdot}OH \quad (9)$$

In the presence of solar light, a steady state concentration of ·OH is achieved and hence the above equation can be reduced to a pseudo-first order reaction [27].

$$-dC_{Ph}/dt = -k_{Ph}.C_{Ph} \quad (10)$$

when t = 0, $C_{Ph} = C_{Ph0}$ the equation is $\ln(C_{Ph}/C_{Ph0}) = -k_{Ph}t$ (11)

As seen from the Eqs. (6)-(8), the phenolics are converted to aromatic and aliphatic intermediates (different organics) and finally mineralized to CO_2. The overall kinetics of phenolic compound degradation can be modeled with respect to dissolved organics (DOC) rather than phenolic compounds. On substituting DOC for C_{Ph} the pseudo-first-order kinetics (Eq. (10) can be written as the Eq. (120 is obtained similar to the work reported [28],

$$\ln DOC_t/DOC_o = -k't \quad (12)$$

where DOC_o and DOC_t are the initial DOC at time = 0 min and the DOC concentration at time 't' min. Pseudo-first-order rate constants (k') represent the overall mineralization reaction and can be obtained through a linear least-square-fit on mineralization data for the phenolic compounds studied as given in Fig. 5. The pseudo-first-order rate constants (k') and their corresponding half-life ($\tau_{1/2}$) are 0.0246 min^{-1} and 28.15 min for phenol; 0.0111 min^{-1} and 62.39 min for TCP; 0.0158 min^{-1} and 43.83 min for TMP and 0.0301 min^{-1} and 23.00 min for TNP respectively. The rate constant for the phenolic compounds studied follows the following order, TNP > Phenol > TMP > TCP.

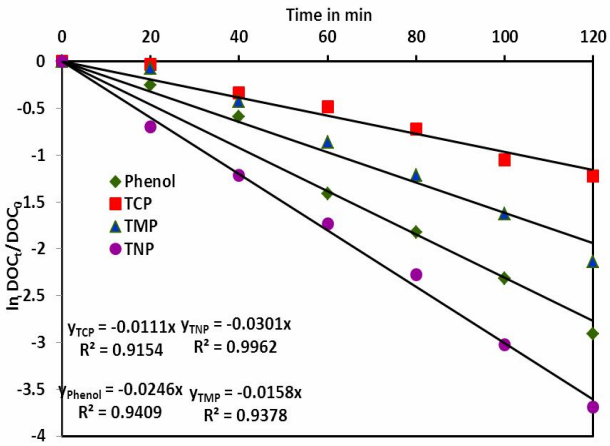

Fig. 5. Kinetics of mineralization for phenol and trisubstituted phenols by heterogeneous process (Experimental conditions were the same as in Fig. 3).

High rate constant is observed for TNP compared to phenol which is due to the presence of electron-withdrawing (EWG) NO_2 group while a low rate constant for TMP is due to the presence of electron releasing groups (ERG), methyl with TCP exhibits the lowest rate constant. To explore further, the effect of EWG or ERG substituent on the reaction kinetics for phenolic degradation, the rate constants are applied to Hammett's equation as shown in Eq. (13)

$$\log(k_{SPh}/k_{Ph}) = \sigma\rho \quad (13)$$

where 'k_{SPh}' and 'k_{Ph}' are pseudo- first-order rate constants for substituted phenols and phenol (regarded as a reference compound) respectively; 'σ' is the Hammett constant and 'ρ' is the reaction constant. Hammett constants (σ) for substituted phenol were calculated as a cumulative sum of σ's for nitro, chloro, and methyl groups at ortho and para positions for TNP, TCP, and TMP respectively. The σ values for TNP, TCP, and TMP were found to be 4.04, 1.59, and -0.43 respectively [29-30]. A positive value of 'σ' indicates the electron-withdrawing nature of -NO_2 and -Cl while the negative value of 'σ' indicates the electron-releasing nature of -CH_3 groups on the aromatic ring [31-32]. A correlation plot between the mineralization rate of substituted phenols (relative to phenol) and σ is presented in Fig. 6. The plot exhibits a poor correlation among nitro, chloro and methyl- substituted phenols while the substituted phenols on degradation proceed through a common stable intermediates namely acetate and oxalate which reflects the reaction may proceed through a common mechanism. But the poor correlation data indicate that the reaction proceeds through a different mechanism with respect to the substituent on the aromatic ring [33].

On substituting the hydrogen of the phenolic ring with three EWG-NO_2 groups (σ = +4.04) as in the case of TNP, the rate constant increases from 2.4 × 10^{-2} min^{-1} to 3.01 × 10^{-2} min^{-1} indicating the aromatic ring is more reactive to hydroxyl attack (·OH). In the presence of 3 EWG-NO_2 groups, the electron density at the *meta* position (with respect to phenolic -OH) is decreased, favoring the hydroxyl attack as shown in the Eq. (14)

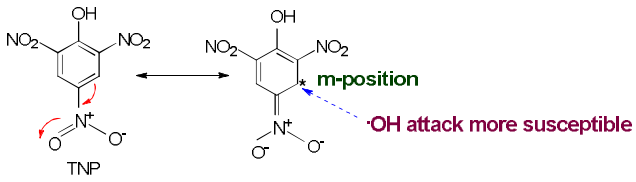

(14)

On substituting the × ring by ERG like -CH_3 groups (σ^- = -0.43) as in the case of TMP, the rate constant decreases to 1.58 × 10^{-2} min^{-1} from 2.4 × 10^{-2} min^{-1} (as in phenol) indicating the degradation reaction is slightly retarded. In TMP, both the phenolic -OH and three methyl groups (occupied at *ortho* and *para* positions) are *o/p* (*ortho/para*) directing, increasing the electron density at the m-position as shown in Eq. (15) thereby making it less susceptible to hydroxyl attack.

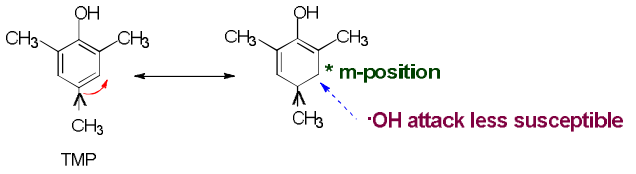

(15)

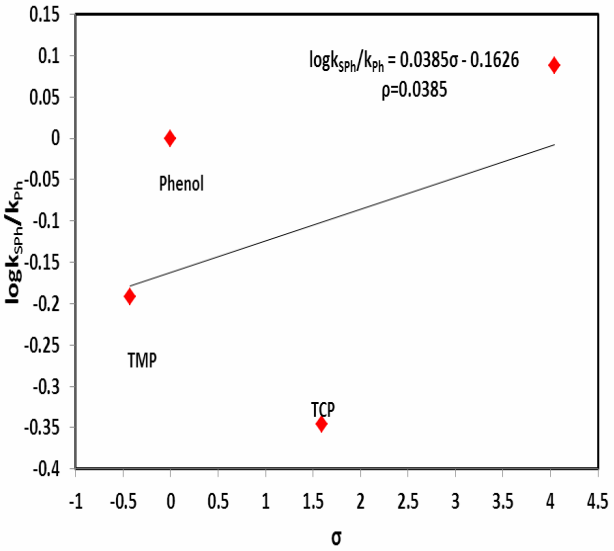

Fig. 6. Correlation between rate constants and the sum of Hammett constants (σ) for substituted phenols by heterogeneous process.

In the case of EWG with deactivating nature like Cl^- (σ^+ = 1.59) as in TCP, the rate constant decreases to 1.11 × 10^{-2} min^{-1} which is lower than with TMP as experienced by Juhee Kim and Ching-Hua Huang [34] during the oxidation of organic compounds with peracetic acid. The degradation reaction is retarded by a factor of 3 as compared with EWG -NO_2. The deactivating nature of the chlorine group is less pronounced in TCP obstructing the attack of a hydroxyl group on the aromatic ring at *m*-position as shown in Eq. (16).

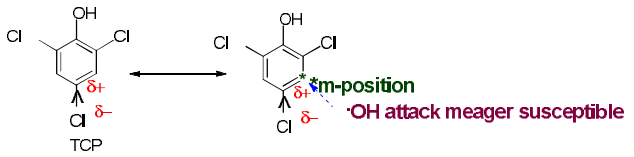

(16)

From the foregoing discussions it is evident that the nature of the substituents greatly influences the hydroxyl attack on the aromatic ring with EWG (meta directors) like -NO_2), the hydroxyl radical attacks at the *m*-positions; EWG with o/p directors like -Cl, the hydroxyl radical attacks the substituents (-Cl) at *o*-position preferentially than at *m*-positions [35] and ERG with *o/p*-directors like -CH_3, the hydroxyl attacks at the substituents (-CH_3) group at *o*-position. It is, therefore, obvious that all the trisubstituted phenols do not follow the same mechanistic pathway which confirms the poor correlation in the Hammett plot.

Mechanism

Kinetics data on mineralization and subsequent analysis on the quantitative structure-activity relationship (QSAR) reveal that the phenolic compounds studied don't follow the same mechanism and provide a plausible reaction pathway for the attack of hydroxyl radical onto the aromatic ring as presented in Fig. 7. The first step in the phenolic degradation process involves the hydrogen abstraction [36] by the hydroxyl radical either on the phenolic ring or on to the substituents. In the case of Phenol (without substituents), the hydrogen abstraction occurs at the *ortho* position to form dihydroxy benzene [catechol, II(a)], with electron-withdrawing groups like -NO_2 onto the phenolic ring (TNP) while the hydrogen abstraction takes place at the

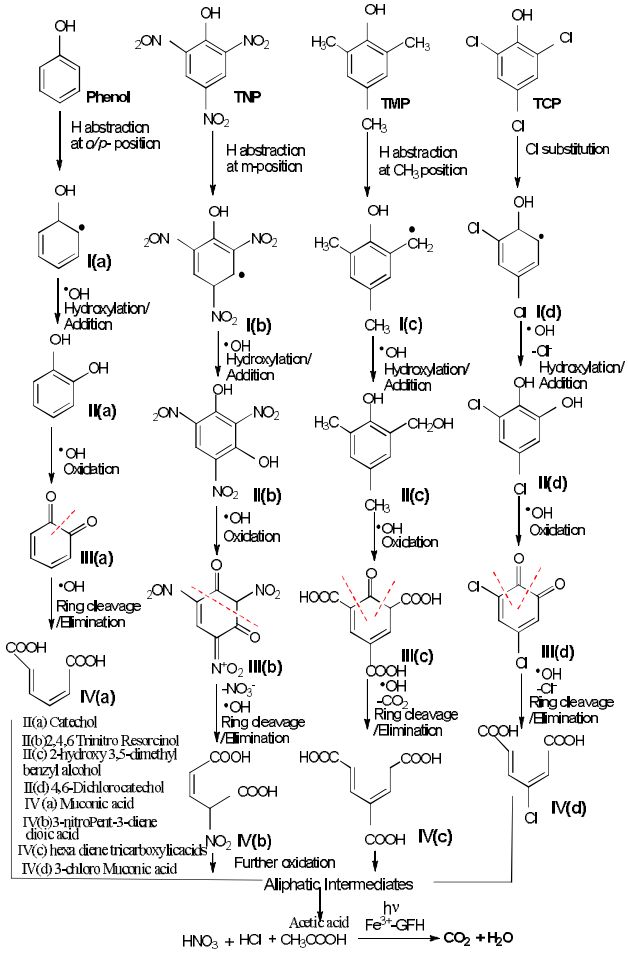

Fig. 7. Possible reaction mechanism for the degradation of phenol and trisubstituted phenols by heterogeneous process.

meta position forming 2,4,6-trinitro resorcinol [II (b)]. In the case of electron-releasing groups like -CH_3, (TMP), the hydrogen abstraction occurs at the methyl substituents to form 2-hydroxy, 3,5-dimethyl benzyl alcohol [II (c)] while with chlorine substituents (TCP), the hydroxyl attack occurs by chlorine substitution to form 2-hydroxy, 3,5-dichloro phenol [II (d)]. The compounds II (a,d) on further oxidation form 1,2-benzoquinone derivatives as in the case of phenol and TCP while 1,3-benzoquinones derivatives with TNP. The *o*-benzoquinone derivatives [III (a,c,d)], on further oxidation undergoes aromatic ring cleavage to form Hexa 2,4-diene, dioic acid (muconic acid derivatives) [IV (a,c,d)].

The m-benzoquinones on oxidation form 3-nitro, pent-3-diene dioic acid which is one carbon atom less than the muconic acid as witnessed in Fig. 3a with the increase in mineralization efficiency within 20 min of the reaction time in TNP. These derivatives [IV (a-d)] on further oxidation undergo further cleavage to form acetate ions whose concentration profiles are presented in Fig. 3b undergoes photochemical oxidation in the presence of GFH at 250-480 nm through ligand to metal charge transfer reactions (LMCT) as shown in Eqs. (1)-(4) contributing for the overall mineralizing of phenolic compounds to CO_2.

CONCLUSIONS

Based on the above results, the following inferences have been obtained, The optimum conditions namely column bed height and flow rate for the recirculating reactor were found to be 5 cm and 210 ml h^{-1} for 2.12 mM of phenol studied. At these optimum conditions, maximum mineralization efficiency of 95% was achieved within 2h of the reaction time indicating the rapid steady-state nature of the flow reactor. The rate of mineralization for the phenolic compounds studied follows pseudo-first-order kinetics and obeys the following sequence, TNP > Phenol > TMP > TCP. The high Mineralization rate for TNP compare to other phenolic compounds is due to the presence of EWG ($-NO_2$). The quantitative structural activity relationship data (QSAR) based on the Hammett plot reveals that the oxidation of phenolic compounds varies widely with the structural diversity. In the presence of EWG ($-NO_2$), the hydroxyl radical attacks the phenolics (TNP) on the aromatic ring, while the ERG ($-CH_3$) and EWG with deactivators (-Cl), the attack of hydroxyl radical takes place on the substituents in the aromatic ring. During the reaction, the presence of acetic acid and inorganic anions namely chloride and nitrate (from TCP and TNP reaction respectively) are identified which suggests the oxidative degradation of phenolic compounds studied.

REFERENCES

[1] Babuponnusami, A.; Muthukumar, K., A review on Fenton and improvements to the Fenton process for wastewater treatment. *J. Environ. Chem. Eng.* **2014**, *2*, 557-572, DOI: 10.1016/j.jece.2013.10.011.

[2] Boruah, P. K.; Sharma, B.; Karbhal, I.; Shelke, M. V.; Das, M. R., Ammonia-modified graphene sheets decorated with magnetic Fe_3O_4 nanoparticles for the photocatalytic and photo-Fenton degradation of phenolic compounds under sunlight irradiation. *J. Hazard. Mater.* **2017**, *325*, 90-100, DOI: 10.1016/j.jhazmat.2016.11.023.

[3] Shukla, P.; Wang, S.; Sun, H.; Ang H. -M.; Tadè Moses., Adsorption and heterogeneous advanced oxidation of phenolic contaminants using Fe loaded mesoporous SBA-15 and H_2O_2. *Chem. Eng. J.* **2010**, *164*, 255-260, DOI: 10.1016/j.cej.2010.08.061.

[4] Catrinescu, C.; Arsene, D.; Apopei, P.; Teodosiu Carmen., Degradation of 4-chlorophenol from wastewater through heterogeneous Fenton and photo-Fenton process catalyzed by Al-Fe PILC. *Appl. Clay Sci.* **2012**, *58*, 96-101, DOI: 10.1016/j.clay.2012.01.019.

[5] Steffi, T.; Anoop Kumar, V.; Vikas, Kumar, S., Synergistic degradation employing photocatalysis and photo-Fenton process of real industrial pharmaceutical effluent utilizing the Iron-titanium dioxide composite. *Process Safety and Environmental Protection* **2021**, *146*, 564-576, DOI: 10.1016/j.psep.2020.11.029.

[6] Hermosilla, D.; Han, C.; Nadagouda, M. N.; Machala, L.; Campo A Gascó, P.; Dionysiou, D. D., Environmentally friendly synthesized and magnetically recoverable designed ferrite photo-catalysts for wastewater treatment applications. *J. Hazard. Mater.* **2020**, *404*, 12120, DOI: 10.1016/j.jhazmat.2019.12120.

[7] Wang, H.; Jing, M.; Wu, Y.; Chen, W.; Ran, Y., Effective degradation of phenol *via* Fenton reaction over CuNiFe layered double hydroxides. *J. Hazard. Mater.* **2018**, *353*, 53-56, DOI: 10.1016/j.jhazmat.2018.03.053.

[8] Ju, L. L.; Chen, Z. Y.; Fang, L. L; Dong, W.; Zheng, F. G.; Shen, M. R., Sol-gel synthesis and photo-fenton-like catalytic activity of $EuFeO_3$ nanoparticles. *J. Am. Ceram. Soc.* **2011**, *94*, 3418-3424, DOI: 10.1111/j.1551-2916.2011.04522.x.

[9] Nie, Y.; Zhang, L.; Li, Y. Y.; Hu, C., Enhanced Fenton-like degradation of refractory organic compounds by

surface complex formation of $LaFeO_3$ and H_2O_2. *J. Hazard. Mater.* **2015**, *294*, 195-200, DOI: 10.1016/ j.jhazmat.2015.03.065.

[10] Krumina, L.; Lyngsie, G.; Tunlid, A.; Persson, P., Oxidation of a dimethoxy hydroquinone by ferrihydrite and goethite nanoparticles: Iron reduction *versus* surface catalysis. *Environ. Sci. Technol.* **2017**, *51*, 9053-9061, DOI: 10.1021/acs.est.7b02292.

[11] Jin, H.; Tian, X.K.; Nie, Y. L.; Zhou, Z. X.; Yang, C.; Li, Y.; Lu, L. Q., Oxygen vacancy promoted heterogeneous fenton-like degradation of ofloxacin at pH 3.2-9.0 by Cu substituted magnetic Fe_3O_4@FeOOH nanocomposite. *Environ. Sci. Technol.* **2017**, *51*, 12699-12706, DOI: 10.1021/ acs.est.7b04503.

[12] Pouran Shima, R.; Abdul Raman, A. A.; Wan, D.; Wan Mohd, A., Review on the application of modified iron oxides as heterogeneous catalysts in Fenton reactions. *J. Clean. Prod.* **2014**, *64*, 24-35, DOI: 10.1016/ j.jclepro.2013.09.013.

[13] Kavitha, V.; Palanivelu, K., Degradation of phenol and trichlorophenol by heterogeneous photo-Fenton process using Granular Ferric hydroxide: comparison with homogeneous system. *Int. J. Environ. Sci. Technol.* **2016**, *13*, 927-936, DOI: 10.1007/s13762-015-0922-y.

[14] Leiduo, L.; Yongli, H.; Hongyu, Z.; Bingkun, H.; Gang, Y.; Bo, L., Critical review of natural iron-based minerals used as heterogeneous catalysts in peroxide activation processes: Characteristics, applications and mechanisms. *J. Hazard. Mater.* **2021**, *416*, 125809, DOI: 10.1016/j.jhazmat.2021.125809.

[15] Wu, Z.; Wang, X.; Zhang, X.; Zhang, Y.; Wang, Y.; Sun, S.; Wu, W. D., Nanostructured semiconductor supported iron catalysts for heterogeneous photo-fenton oxidation: A Review. *J. Mater. Chem. A.* **2020**, *30*, 15513-15546, DOI: 10.1039/D0TA04541A.

[16] Cui, L.; Xiaoxun, S.; Ling, L.; Min, C.; Xigui, L.; Shiyu, L.; Bisheng, L.; Huan, Y.; Lei, Q.; Mingming, Z.; Ning, A., Enhancing iron redox cycling for promoting heterogeneous Fenton performance: A review. *Sci. Total Environ.* **2021**, *775*, 145850, DOI: 10.1016/j.scitotenv. 2021.145850.

[17] Nishanth, T.; Dionysios, D. D.; Suresh, C. P., Heterogeneous fenton catalysts: A review of recent advances. *J. Hazard. Mater.* **2020**, *404*, 124082, DOI: 10.1016/j.jhazmat. 2020.124082.

[18] Meng-hui, Z.; Hui, D.; Liang, Z.; De-xi, W.; Di, M., A review on Fenton process for organic wastewater treatment based on optimization perspective. *Sci. Total Environ.* **2019**, *670*, 110-121, DOI: 10.1016/j.scitotenv.2019.03.180.

[19] Hussain, S.; Aneggi, E.; Goi, D., Catalytic activity of metals in heterogeneous Fenton-like oxidation of wastewater contaminants: a review. *Environ. Chem Lett.* **2021**, *19*, 2405-2424, DOI: 10.1007/ s10311-021-01185-z.

[20] Khana, I.; Nomuraa, E.; Kuzmann, B.; Homonnayb, Z.; Sinkób, K.; Ristić, M.; Krehulac, S.; Musić, S.; Kubukia, S., Photo-Fenton catalytic ability of iron-containing aluminosilicate glass prepared by sol-gel method. *J. Alloys Compd.* **2020**, *816*, 153-163, DOI: 10.1016 /j.jallcom. 2019.153227.

[21] Bansal, P.; Verma, A., Synergistic effect of dual process (photocatalysis and photo-Fenton) for the degradation of Cephalexin using TiO_2 immobilized novel clay beads with waste fly ash/foundry sand. *J. Photochem. Photobiol. A Chem.* **2017**, *342*, 131-142, DOI: 10.1016/ j.jphotochem. 2017.04.010.

[22] Adish Kumar, S.; Sree lekshmi, G. S.; Rajesh Banu, J.; Tae Yeom, I., Synergistic degradation of hospital wastewater by solar/TiO_2/Fe^{2+}/H_2O_2 process. *Water Qual. Res. J. Canada.* **2014**, *49*, 223-233, DOI: 10.2166/wqrjc.2014.026.

[23] Demir, M. E.; Chehade, G.; Dincer, I.; Yuzer, B.; Selcuk, H., Synergistic effects of advanced oxidization reactions in a combination of TiO_2 photocatalysis for hydrogen production and wastewater treatment applications. *Int. Hydrogen Energy.* **2019**, *44*, 23856-23867, DOI: 10.1016/j.ijhydene. 2019.07.110.

[24] Wendong, F.; Yunhai, W.; Jian, L.; Kai, G.; Hongxiang, A., Decomposition of spent radioactive ion-exchange resin using photo-fenton process. *J. Chem. Technol. Biotechnol.* **2020**, *95*, 2522-2529, DOI: 10.1002/jctb.6437.

[25] Hermosilla, D.; Merayo, N.; Gasco, A.; Blanco, A., The application of advanced oxidation technologies to the treatment of effluents from the pulp and paper industry: a review. *Environ. Sci. Pollut. Res.* **2015**, *22*, 168-191, DOI: 10.1007/ s11356-014-3516-1.

[26] Joao˜ Peres, R.; Maria Isabel, N., Recent trends and developments in Fenton processes for industrial wastewater treatment- A critical review. *Environ. Res.* **2021**, *197*, 110957, DOI: 10.1016/j.envres.2021.110957.

[27] Soriano-Molina, P.; Miralles-Cueva, S.; Esteban Garc´ıa, P.; Plaza-Bolanos, B.; Sanchez, P.; P´ erez, J. A., Two strategies of solar photo-Fenton at neutral pH for the simultaneous disinfection and removal of contaminants of emerging concern. Comparative assessment in raceway pond reactors. *Catalysis Today* **2019**, *361*, 17-23, DOI: 10.1016/j.cattod.2019.11.028.

[28] Yu L.; Hefa, C., Chemical kinetic modeling of organic pollutant degradation in Fenton and solar photo-Fenton processes. *Journal of the Taiwan Institute of Chemical Engineers* **2021**, *123*, 175-184, DOI: 10.1016/j.jtice.2021.05.011.

[29] Lee, Y.; von Gunten, U., Quantitative structure-activity relationships (QSARs) for the transformation of organic micro-pollutants during oxidative water treatment. *Water Res.* **2012**, *46*, 6177-6195, DOI: 10.1016/j.watres.2012.06.006.

[30] Ye, T.; Wei, Z.; Spinney, R.; Dionysiou, D. D.; Luo, S.; Chai, L.; Yang, Z.; Xiao, R., Quantitative structure-activity relationship for the apparent rate constants of aromatic contaminants oxidized by ferrate(VI). *Chem. Eng. J.* **2017**, *317*, 258-266, DOI: 10.1016/j.cej.2017.02.061.

[31] Pavithra Bhakthi, J.; Gayani Chathurika, P.; Athula, B.; Nalaka Deepal, S.; Nadeeshani, N., Theoretical study of phenol and hydroxyl radical reaction mechanism in aqueous medium by the DFT/B3LYP/6-31+G(d,p)/CPCM model. *Can. J. Chem.* **2014**, *92*, 809-813. DOI: 10.1139/cjc-2014-0191.

[32] Xi, H.; Qun, Z.; Yang, Z.; Qingxuan, Z.; Xianfeng, W.; Chaoyang, Z., A DFT study toward the reaction mechanisms of TNT with hydroxyl radicals for advanced oxidation processes. *J. Phys. Chem. A.* **2016**, *120*, 3747-3753, DOI: 10.1021/acs.jpca.6b03596.

[33] Giovanni, P.; Maurizio, A.; Vincenzo, A.; Tullio Caronna Agatino Di, P.; Elisa Garcı´a, L.; Vittorio, L.; Giuseppe, M.; Leonardo, P.; Mario, S., Selectivity of hydroxyl radical in the partial oxidation of aromatic compounds in heterogeneous photocatalysis. *Catal. Today* **2007**, *122*, 118 -127, DOI: 10.1016/j. cattod. 2007.01.026.

[34] Juhee, K.; Ching-Hua, H., Reactivity of peracetic acids with organic compounds: A critical review. *ACS EST Water* **2021**, *1*, 15-33, DOI: 10.1021/acsestwater.0c00029.

[35] Francis, A. C.; Richard, J. S., Advanced Organic Chemistry, Part A: Structure and Mechanisms. Springer Press: **2007**, pp. 335-345.

[36] Yang, Z.; Xiaoqiang, L.; Weidong, J.; Yuanjie, S., Theoretical insight into reaction mechanisms of 2,4-dinitroanisole with hydroxyl radicals for advanced oxidation processes. *J. Mol. Model.* **2018**, *24*, 44 -52, DOI: 10.1007/s00894-018-3580-4.